

# QUALIFICATION AND IMPROVEMENT OF IRON ENDF/B-VI AND JEF-2 EVALUATIONS BY INTERPRETATION OF THE ASPIS BENCHMARK

S.H. ZHENG - I. KODELI - C. RAEPSAET  
C.M. DIOP - J. C. NIMAL - A. MONNIER

*COMMISSARIAT A L'ENERGIE ATOMIQUE  
CENTRE D'ETUDES NUCLEAIRES DE SACLAY  
DMT/SERMA/LEPP  
91191 GIF SUR YVETTE CEDEX  
FRANCE*

## INTRODUCTION

The aim of the present study is to contribute to the validation of the new evaluated nuclear data files like ENDF/B-VI (distr. 90) or JEF-2.2.

The new cross-section evaluations for iron isotopes are of particular interest for the nuclear community, since it is well known that the ENDF/B-IV data underestimate the neutron flux on deep penetration problems. The performances of the new nuclear data libraries are compared with those of ENDF/B-IV. The ASPIS benchmark, where the neutron transports through more than one meter iron plate, was chosen for this study.

The cross-section libraries were produced by the THEMIS/NJOY (ref 1) processing system and the transport calculations were carried out using the 3D Monte Carlo code TRIPOLI (ref 2). The influence of different multigroup cross-section representations was investigated.

Finally, sensitivity, uncertainty and data adjustment analyses were carried out to obtain some additional informations about the quality of the cross-section data in ENDF/B-VI files. The analyses were performed using the code package set up of different modules, either developed at CEA or obtained from the NEA Data Bank. The adjustment indicated that some modifications have to be introduced to the neutron cross-sections of iron and the whole calculations were repeated with the adjusted set of cross sections.

The comparison of the results of the uncertainty and the adjustment analyses applied to ENDF/B-IV and ENDF/B-VI iron data permits to establish the progress made and gives some indications about the state-of-the-art of the cross section data.

## DESCRIPTION OF THE EXPERIMENT

The ASPIS experiment on neutron deep penetration in iron has been carried out at Winfrith to contribute to the OECD (NEA) Collaborative Benchmark Exercise on assessing the nuclear data requirements for radiation shielding.

The details of the ASPIS experiment are described in ref 3 and 4. It consists of a low-power natural uranium converter plate, driven by the source reactor NESTOR, a graphite moderator

and an extensive iron shield. This iron shield is composed by 24 mild steel plates, each 1830 mm wide, 1910 mm high and 50.8 mm thick. A 6.35 mm simplified air gap between adjacent plates allows the location of the detectors.

A cylindrical model (from ref 3) with rectangular members shown as equal area cylinders is used for the calculation (fig 1); in the iron shield, the steel has been stretched to fill the 6.35 mm air gap and the steel density has accordingly been reduced by a factor 0.889. The detectors,  $Rh_{103}(n,n')Rh_{103}^m$ ,  $In_{115}(n,n')In_{115}^m$  and  $S_{32}(n,p)P_{32}$  are used to measure the reaction rates on the axes of iron shield.

## CALCULATIONAL METHOD AND CROSS SECTIONS

The calculations were realized using the 3 dimensional Monte Carlo code TRIPOLI (ref 2), which solves the Boltzmann integral transport equation, which governs the neutron propagation in the matter.

In the TRIPOLI code, the general geometry is exactly described using equations of the first and second order. The biasing technics are used to accelerate the simulation, specially in the neutron deep penetration cases.

The neutron cross sections are given in a multigroup representation by the THEMIS/NJOY system (ref 1) as follows :

$$\sigma_{xg} = \frac{\int_{E_g}^{E_{g+1}} \sigma_x(E) \mathcal{F}(E) dE}{\int_{E_g}^{E_{g+1}} \mathcal{F}(E) dE}$$

where x is the reaction type, g the group number and  $\mathcal{F}$ , the weight function.

The cross section libraries ENDF/B4, ENDF/B6 (distr. 90) and JEF 2.2 have been used and processed with the following multigroup representations :

- 315 group structure ( $\Delta u \approx 1/20$  in the region of interest) weighted by a fission spectrum for  $E > 1$  MeV, and by  $1/(E \cdot \Sigma_t(E))$  for the energy below 1 MeV, where  $\Sigma_t(E)$  is the total macroscopic cross section of the composition.
- 3857 group structure ( $\Delta u \approx 1/480$  for  $E > 9$  keV) with the same weight function.
- 315 group structure represented by a probability table method (ref 5 and 6).
- 315 group adjusted cross sections.

The cross sections of the 3 detectors used during the calculation are taken from the IRDF85 library. Their thresholds are 100 keV for  $Rh_{103}$ , 300 keV for  $In_{115}$  and 1 MeV for  $S_{32}$ .

## SENSITIVITY AND ADJUSTMENT ANALYSES

The principal sources of the uncertainty in the neutron fluence calculations are :

- mathematical methods (numerics, group collapsing, transport calculation),
- geometry and material composition uncertainties and simplifications used in the calculational model,
- cross sections and other nuclear data uncertainties,
- neutron / gamma source strength uncertainties.

Assuming the error introduced by the calculational method itself is negligible, the uncertainty in the calculated flux can be reduced by adjustment. A least square method is normally adopted. Data adjustment requires the measured and the calculated integral results, the sensitivity profiles of the integral results to the nuclear data, as well as a covariance matrix of both the basic nuclear data and the measured integral data. In so far as the data are well compatible, the expected uncertainties in the adjusted parameters are substantially smaller than those in the unadjusted library.

The sensitivity and adjustment analyses were performed using a code package (ref 7) set up of different modules, either obtained from the NEA-Data Bank or developed at CEA. The calculational scheme used is presented in another paper at this conference (ref 8, Table 2). The sensitivity profiles are calculated using the SUSD code (ref 9) in conjunction with the one- and two-dimensional  $S_N$  transport codes ANISN and TWODANT (ref 10, 11, 12). ZOTT code (ref 12) is used for the adjustment. The covariance matrices were taken from the ZZ-VITAMIN-J/COVA library (ref 13). The linear perturbation method is adopted.

To limit the covariance matrices and the number of parameters used in the adjustment to a reasonable size, rather broad 30 group ENDF/B-IV based cross-sections were adopted in the ANISN and TWODANT calculations. It is obvious that for an accurate description of the absolute flux in a deep penetration problem like ASPIS this is not sufficient, because the errors due to the cross-section processing (group collapsing, self-shielding treatment) become increasingly important with the distance. On the other hand the sensitivity profiles as relative quantities were expected to be less affected by these errors.

The 30 group transport calculations served therefore only to determine the relative sensitivity profiles of the  $R_h$ ,  $I_n$  and  $S$  reaction rates at the different penetrations in iron, to the iron cross-sections and the response functions. The TRIPOLI Monte-Carlo code calculations, performed in 315 and 3857 energy groups, provided the reference calculated reaction rates for the adjustment. The adjustment was nevertheless restricted to the penetration of less than 65 cm, since the data processing error has increasing impact on the sensitivity calculations, as well as on the 315 group neutron flux calculations.

The principal objective was to adjust the iron cross-sections on the basis of the calculated and measured  $R_h$ ,  $I_n$  and  $S$  reaction rates. The TRIPOLI code was then rerun using the adjusted sets of cross-sections and the results were compared to the reaction rates from the original calculation.

The adjustment was first applied to the C/E values obtained using the standard 315 energy group calculation. The comparison to the 3857 group and probability table calculations (table 1) shows that these values (in particular  $I_n$  reaction rates) are subject to a non-negligible data processing error at large distances. The adjustment gives nevertheless reasonable results for the  $I_n$  and  $S$  reaction rates which are significantly improved. The  $R_h$  reaction rates on the other hand look marginally better at larger distances, but only on the cost of an overestimation at smaller distances. It is though evident that the adjustment factors partly account for the cross-section processing error. In this way these adjustments should be considered as valid only for the specific applications, which do not differ significantly from ASPIS experiment and where a similar energy group structure and cross-section processing are used. The adjustment is mathematically not rigorous, since the C/E values are not completely consistent with the input covariance data, which contain only the data evaluation uncertainties.

The adjustment performed on the basis of the reaction rates, calculated using the probability tables, clearly demonstrates this fact. As the cross-section processing errors have been reduced considerably, the adjustment factors correct primarily the data evaluation errors. The nonelastic cross-section adjustments above 3 MeV remain practically the same as in the 315 group

adjustment, but are substantially different below. It is immediately clear that the difference is due to the fact that the 315 group adjustment factors in this region reflect the errors due to the use of the coarse group structure and the absence of self-shielding.

Figure 2 and 3 present the adjustments for the iron ENDF/B-IV and ENDF/B-VI cross-sections, obtained adopting the same procedure to the ENDF/B-VI probability table results. The factors are preliminary, since they are based on the sensitivity profiles from the ENDF/B-IV calculations. The covariance matrices of the Fe-56 isotope were used.

## RESULTS

The comparison between the experimental and calculational results are given in table 1 and figure 4. The experimental systematic errors are 3% for Rh, 2% for In and 4% for S. The statistical errors in the calculational reaction rates are 4% for Rh, 5% for In and 3% for S.

ENDF/B4 results : from the results of the calculation with non adjusted ENDF/B4, we can conclude that a 315 group structure is not sufficient to process deep penetration problems for neutrons. The results are improved with probability tables and 3857 group structure. The 3857 group calculation gives a negligible error due to the energy group collapsing. The results and the adjusted coefficient show that the nonelastic cross section was overestimated in this library over 1 MeV.

ENDF/B6 results : for the 3857 group structure and the probability tables, the In and S results are in good agreement with the experiment, but the Rh reaction rates are really different. A 3857 group structure could somehow be unsufficiently precise to represent the Rhodium cross section in that energy range.

JEF-2 results : the results obtained are different from measurements. If we compare the JEF-2 and ENDF/B6 cross sections for Fe<sup>56</sup>, we can see that the first excited level of the inelastic scattering is systematically 0,1 barn less in JEF-2 than in ENDF/B6. This has a direct influence on the S32 response, for  $E > 2$  MeV. The results for Rh and In are more difficult to explain. However, the source is described as a fission spectrum ( $E \approx 2$  MeV). As the first inelastic level is underestimated in JEF-2, the flux in the energy range  $E' = E_{\text{source}} - E_{\text{first level}}$ , which is In and Rh energy range, is underestimated too.

## ACKNOWLEDGMENTS

Thanks are due to P. Ribon for his appreciable contribution and his help, specially concerning the probability tables.

## CONCLUSIONS

The uncertainty and adjustment analyses proved to be of great value for the validation of the neutron transport calculations. The adjustment indicated the needs for some modifications to be introduced to the neutron cross sections of iron. The results obtained with this adjusted sets of data show considerably improved agreement between the calculation and the experiment.

14090016

Before adopting the adjusted results, one must be well aware of their limitations. In particular, one must pay attention to the following:

- The fundamental restriction is the quality of the covariance (uncertainty) information. It is evident that the quality of the adjusted data cannot be better than the quality of the input covariance data and that the deficiencies in the covariance information can lead to completely erroneous conclusions.
- The processing of the data (e.g. cross section group averaging, self shielding treatment, etc.) introduces additional errors, which are sometimes difficult to take into account properly. These errors are in addition peculiar to a specific problem, which makes the results of the adjustment to some extent problem dependent. In order to obtain the good set of data for general use it is therefore of prime interest to reduce this data processing errors to a minimum.
- Linear perturbation methods are usually used for the sensitivity and adjustment analyses. This implies the linear dependence between the target quantity and the basic data. This approximation is valid if the uncertainties and the data correction factors are relatively small.

## References

- 1 - C. Raepsaet, C. Diop et al : *The THEMIS/NJOY processing system*, CEA to be published
- 2 - J. C. Nimal, A. Baur, D. Dejonghe, J. Gonnord, A. Monnier, T. Vergnaud : *TRIPOLI : Energy dependant three dimensional Monte Carlo program* ORNL - OLS - 80 110 (1980)
- 3 - J. Butler et al. : *Results and calculational Model of the Winfrith Iron Benchmark*, NEACRP-A-629
- 4 - A. K. McCracken : *The establishment of a shielding experimental benchmark at the NEA Data Bank*, NEACRP-A-1044, June 1990
- 5 - P. Ribon et al. : *Les tables de probabilités, application au traitement des sections efficaces pour la neutronique*, CEA to be published
- 6 - S.H. Zheng et al. : *The Monte Carlo transport calculations using the probability tables method for cross sections*, CEA to be published
- 7 - I. A. Kodeli, et al., *Uncertainty and Data Adjustment Analyses for PWR Shielding*, ANS Topical, M&C, Pittsburg, 1991.
- 8 - I. A. Kodeli, E. Sartori, *Experience with Collapsing and Expanding Multi-group Cross-section Covariance Matrices*, presented at this conference.
- 9 - K. Furuta et al., *SUSD: A Computer Code for Cross Section Sensitivity and Uncertainty Analyses Including Secondary Neutron Energy and Angular Distributions*, UTNL-R-0185, 1986.
- 10 - W. W. Engle Jr., *A Users Manual for ANISN*, Report ORNL/K-1693, ORNL, 1967.
- 11 - R. E. Alcouffe, et al., *Users Guide for TWODANT: A Code Package for Two-Dimensional, Diffusion-Accelerated, Neutral-Particle Transport*, LA-10049-M, LANL, 1989.
- 12 - D. W. Muir, *Evaluation of Correlated Data using Partitioned Least Squares: A Minimum-Variance Derivation*, Nucl. Sci. Eng: 101, p88 (1989).
- 13 - I. A. Kodeli, E. Sartori, *Covariance Data Library ZZ-VITAMIN-J/COVA*, NEA Data Bank package 1264/03, 1990.

315 group structure						3857 group structure			Probability tables 315 group structure						d (cm)	
Rh 103		In 115		S 32		Rh 103	In 115	S 32	Rh 103	In 115		S 32				
n adj	adj	n adj	adj	n adj	adj	n adj	n adj	n adj	n adj	adj	n adj	adj	n adj	adj		
ENDF/B4																
0.89	0.92	0.97	1.03	0.92	0.99	0.89	1.00	0.95	0.85	0.87	0.97	1.00	0.92	0.95	5.72	
0.96	0.98	0.94	0.99	0.89	1.01	0.94	0.99	0.93	0.92	0.92	0.98	0.98	0.91	0.97	11.43	
0.99	1.04	0.90	0.98	0.91	1.01	0.96	0.92	0.96	0.96	0.93	0.96	0.92	0.92	0.98	17.15	
0.99	1.01	0.89	1.00	0.84	1.01	0.96	0.99	0.88	0.93	0.94	0.95	1.00	0.88	0.96	22.86	
1.03	1.07	0.95	1.05	0.82	1.00	1.03	0.99	0.85	0.98	1.01	1.00	1.00	0.87	0.95	28.58	
1.04	1.10	0.88	1.07	0.79	1.06	1.06	1.04	0.84	1.05	1.02	1.09	1.06	0.85	0.95	34.29	
				0.79	1.05			0.85					0.86	1.00	40.01	
1.06	1.18	0.81	1.05	0.72	1.05	1.09	0.98	0.81	1.12	1.07	1.05	1.03	0.82	0.97	45.72	
1.02	1.09	0.76	0.91	0.72	1.02	1.07	0.95	0.84	1.09	1.04	1.01	0.98	0.84	0.96	51.44	
1.00	1.09	0.75	0.95	0.62	0.93	1.06	0.97	0.72	1.11	1.04	1.10	1.04	0.77	0.90	57.15	
0.92	1.05	0.72	0.93	0.63	0.99	1.04	1.02	0.78	1.06	0.99	1.12	1.02	0.82	0.97	62.87	
0.91	1.06			0.52	0.86	1.07		0.73	1.10	1.07			0.73	0.86	68.58	
0.89	0.99					1.05			1.12	1.05					74.30	
0.74	0.86					1.02			1.03	1.01					85.73	
0.69	0.81					0.96			1.03	0.99					91.44	
0.51	0.65					0.84			0.88	0.88					102.87	
0.43	0.56					0.82			0.85	0.85					114.30	

ENDF/B6									
0.92	1.05	1.02	0.86	0.85	0.99	0.97	1.00	0.98	5.72
0.96	1.02	1.05	0.95	0.91	1.05	0.97	1.03	1.02	11.43
0.97	0.95	1.09	0.95	0.96	0.98	0.95	1.09	1.06	17.15
0.99	1.02	1.06	0.94	0.93	1.03	0.99	1.05	1.02	22.86
1.06	1.08	1.07	0.97	0.97	1.03	1.06	1.10	1.01	28.58
1.09	1.09	1.05	1.09	1.04	1.12	1.10	1.08	1.03	34.29
		1.08					1.16	1.08	40.01
1.16	1.03	1.05	1.11	1.06	1.08	1.03	1.10	1.01	45.72
1.16	1.02	1.05	1.05	1.06	1.02	1.01	1.14	1.03	51.44
1.19	1.06	0.97	1.10	1.06	1.15	1.04	1.02	0.95	57.15
1.17	1.01	1.10	1.08	1.05	1.07	1.03	1.15	1.06	62.87
1.28		0.93	1.15	1.12			1.00	0.96	68.58
1.26			1.10	1.12					74.30
1.30			1.13	1.10					85.73
1.36			1.14	1.13					91.44
1.22			1.00	0.99					102.87
1.26			1.05	1.06					114.30

JEF 2							
0.90	1.05	1.01	0.86		0.98	1.02	5.72
0.90	0.99	1.06	0.88		0.94	1.10	11.43
0.90	0.93	1.13	0.91		0.91	1.19	17.15
0.91	0.95	1.11	0.93		0.89	1.19	22.86
0.93	0.94	1.13	0.89		0.89	1.18	28.58
0.94	0.93	1.15	0.88		0.85	1.23	34.29
		1.26				1.32	40.01
0.96	0.80	1.22	0.90		0.72	1.31	45.72
0.93	0.75	1.26	0.88		0.63	1.35	51.44
0.92	0.72	1.20	0.89		0.66	1.28	57.15
0.89	0.71	1.34	0.85		0.62	1.49	62.87
0.92		1.19	0.89			1.29	68.58
0.89			0.88				74.30
0.86			0.87				85.73
0.85			0.88				91.44
0.75			0.77				102.87
0.74			0.77				114.30

**Table 1 :**

C/E values for the 3 detectors versus the thickness of the iron slab

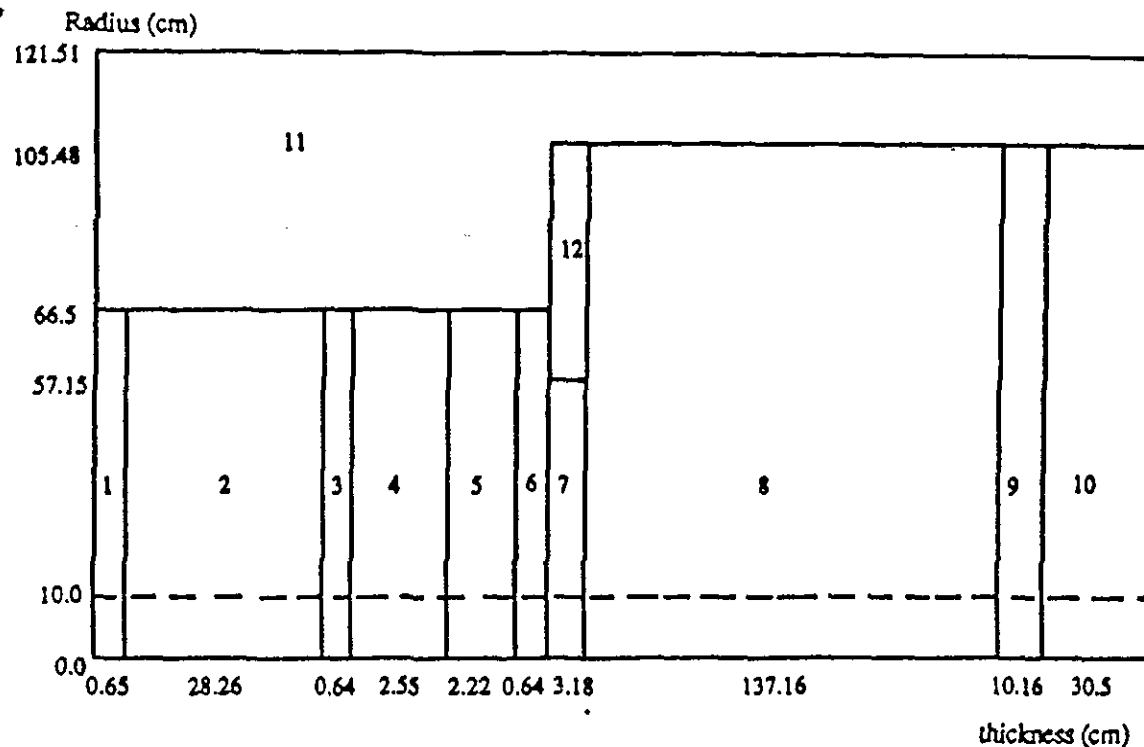
C : TRIPOLI results  
E : Experimental results  
d : thickness  
n adj : calculation with non adjusted cross sections  
adj : calculation with adjusted cross sections

Table 1 :

C/E values for the 3  
detectors versus the  
thickness of the iron slab

C: TRIPOLI results  
E: Experimental results  
d: thickness  
n adj: calculation with non  
adjusted cross  
sections  
adj: calculation with  
adjusted cross  
sections

14090018



**Figure 1 :** Calculational geometry of the Benchmark ASPIS  
 1, 3, 7 : Aluminium; 2 : Carbone; 4, 6 : Air; 5 : Converter plate  
 8 : Iron shield; 9, 12 : Mild Steel; 10, 11 : Concrete

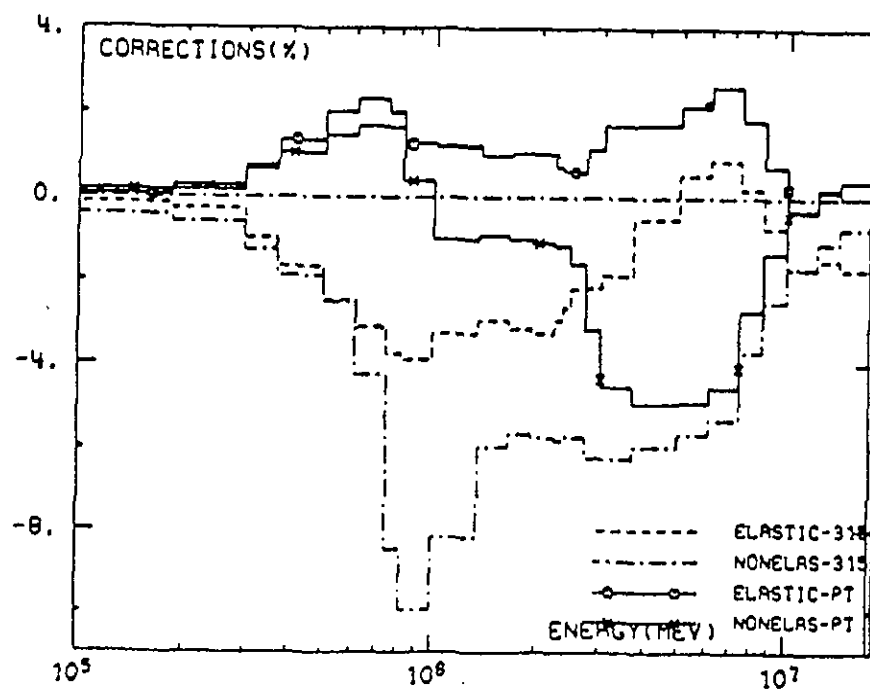


**Figure 2 :** Adjustment of the iron cross section  
 (ASPIS experiment)

14090019

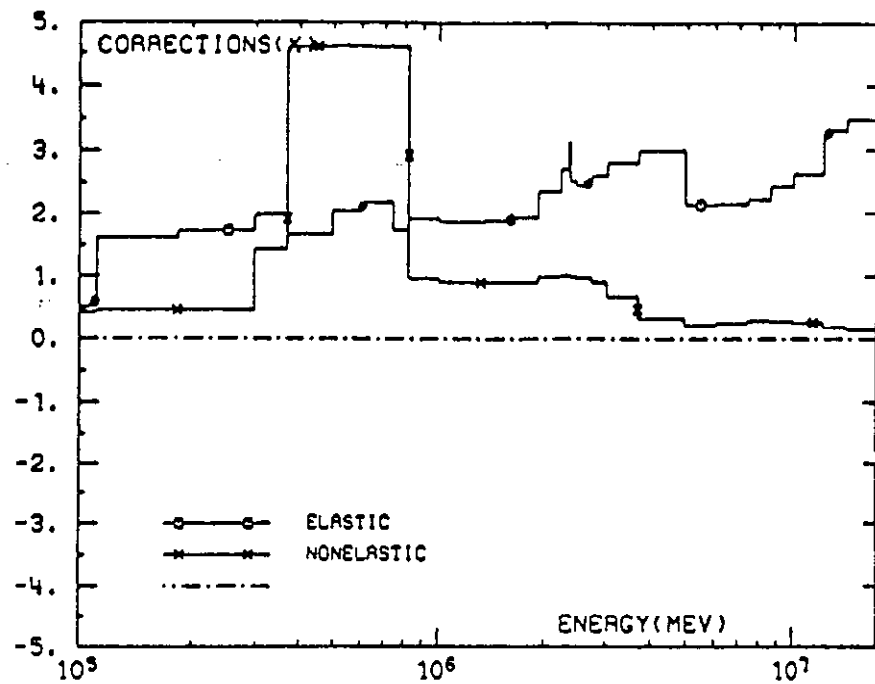


**Figure 3 :** Adjustment of Fe56 ENDF/B6 cross sections (ASPIS experiment - probability tables)

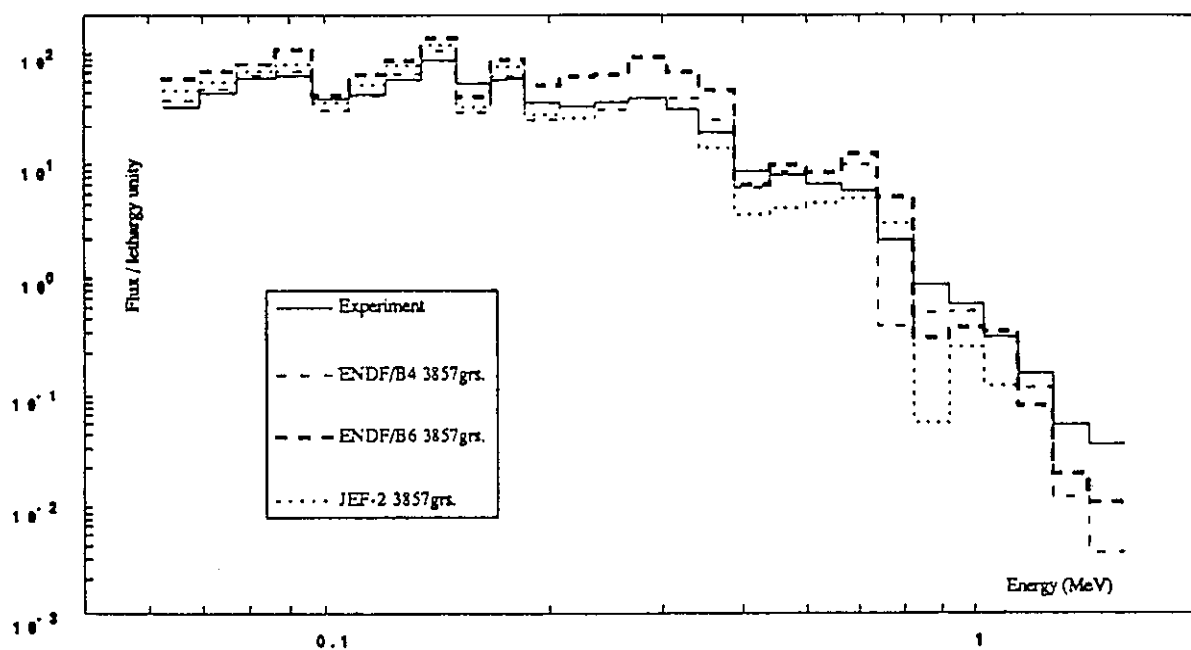


**Figure 4 :** TRIPOLI and experimental neutron spectra at 114,3 cm

14090020